

Hydrogen Bonding Induced Supramolecular Self-Assembly of Linear Doubly Discotic Triad Supermolecules

Jianjun Miao^[a] and Lei Zhu^{*[a, b]}

Abstract: A series of linear doubly discotic triad supermolecules based on a porphyrin (P) core and two triphenylene (Tp) arms linked by amide bonds are synthesized. The samples are denoted as P(Tp)₂. Hydrogen bonding along the P stacks is the primary driving force for the supramolecular self-assembly of P(Tp)₂ triad supermolecules. Meanwhile, the degree of coupling between P and Tp disks also

plays an important role. For samples with the spacer lengths longer than or similar to the alkyl chain lengths in the Tp arms, P and Tp are decoupled to a large degree. This decoupling result in non-uniform tilt angles for P and Tp

Keywords: hydrogen-bonding · porphyrins · self-assembly · supermolecular chemistry · triphenylene

disks along both the *a*- and *c*-axes. Therefore, large unit cells are observed with eight P(Tp)₂ supermolecules per cell. For a sample with the spacer length much shorter than the alkyl chains in the Tp arms, P and Tp are strongly coupled. Therefore, both P and Tp have uniform tilt angles along the *a*- and *c*-axes. A small unit cell is obtained with only one P(Tp)₂ supermolecule per cell.

Introduction

Supramolecular self-assembly is mainly governed by the non-covalent interactions, such as van der Waals interactions, π - π interactions, or hydrogen bonding as well as molecular shape/topology, space-filling effects, and microsegregation of incompatible parts of the constituent molecules.^[1] On the other hand, supermolecules are comprised of well-defined, covalently linked small molecular moieties with multi-functions, and thus represent a novel class of advanced functional materials, which can further self-assemble into hierarchical structures.^[2] Liquid crystalline (LC) supermolecule-stabilized non-covalent interactions are particularly interesting, because their supramolecular self-assembly can

enhance the functionality of individual LC molecules,^[2,3] and the resultant unique physical properties are attractive for applications in advanced optoelectronic materials and biology.^[3-9]

Among LC supermolecules, calamitic polypeptide LC supermolecules have received much research attention.^[10-36] However, discotic LC polypeptides containing three or more discotic mesogenic units have not been as extensively studied as calamitic LC polypeptides.^[37,38] A variety of molecular architectures for discotic LC polypeptides have been made possible, e.g., linear,^[39-41] star-shaped,^[42-49] and mixed calamitic/discotic.^[50-52] For most linear and star-shaped discotic LC polypeptides, a normal hexagonal columnar phase with the unit cell dimension close to that of the parent triphenylene (Tp) and hexa-*peri*-hexabenzocoronene (HBC) discotic LCs was observed, suggesting that the peripheral Tp or HBC discotic mesogens self-organized into individual LC columns regardless of the covalent linkages to the central core. However, for mixed calamitic/discotic triads, unconventional meso-scale self-assembly (e.g., nematic columnar phases) was observed with a specific arrangement of the calamitic mesogens with respect to the LC columns.

In addition to the shape and topology, hydrogen bonding is another important determining factor for the supramolecular self-assembly of discotic LC supermolecules. An elegant example of hydrogen bond-induced columnar liquid crystals (LCs) in an otherwise non-liquid crystalline discotic molecule is 1,3,5-benzenetrisamides.^[53-56] A C₃-symmetry was ob-

[a] J. Miao, Prof. L. Zhu

Polymer Program, Institute of Materials Science and Department of Chemical, Materials and Biomolecular Engineering
University of Connecticut
Storrs, Connecticut 06269-3136 (USA)
Fax: (+1) 216-368-4202
E-mail: lxz121@case.edu

[b] Prof. L. Zhu

Department of Macromolecular Science and Engineering
Case Western Reserve University
Cleveland, Ohio 44106-7202 (USA)

Supporting information for this article is available on the WWW under <http://dx.doi.org/10.1002/asia.201000017>.

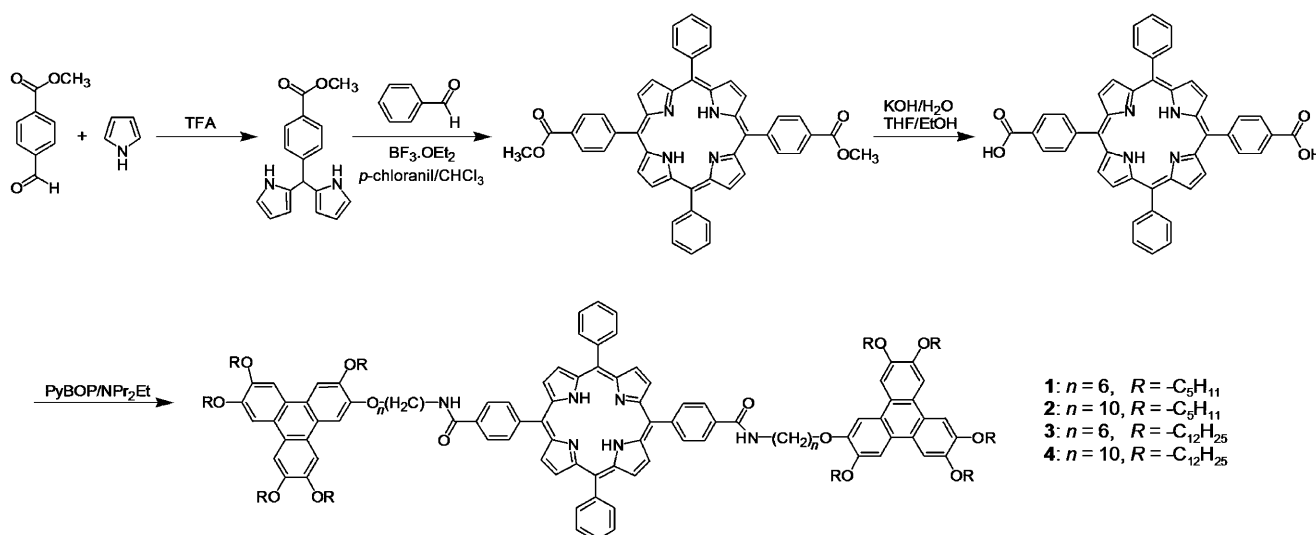
served within a column, where the 120° rotation between neighboring benzenetrisamide molecules was stabilized by intermolecular hydrogen-bonding along the column direction. Meanwhile, a sergeants-and-soldiers principle was presented by Meijer et al. in these systems.^[57–59] The discotic LC phases induced by hydrogen bonding showed a higher thermal stability and better responses to external stimuli such as electric and magnetic fields.^[60,61] Paraschiv et al. reported a series of 1,3,5-benzenetrisamide with three pendent hexaalkoxytriphenylene groups by varying the spacer length and the Tp arm length.^[62,63] Four columnar hexagonal phases were identified in total, where intermolecular hydrogen bonds connected the central benzene cores in such a way that the adjacent benzene cores rotated 120° apart, therefore leading to a helical orientation of the resulting columnar stacks. A high mobility of 0.23 cm²V⁻¹s⁻¹ was found in one of those Tp benzenetrisamide samples.^[63]

In this work, we synthesized a series of doubly discotic triads based on a porphyrin (P) central core and two Tp arms linked by amide bonds. These samples, denoted as P(Tp)₂, are different from the doubly discotic supermole-

cules in a previous report [one P core with four Tp arms linked by amide bonds, denoted as P(Tp)₄],^[64] because P(Tp)₂ has a C₂ symmetry and P(Tp)₄ has a C₄ symmetry. Experimental results showed that hydrogen bonding along the P stacks induced crystalline phases for P(Tp)₂, rather than the discotic LC phases for P(Tp)₄. In addition to hydrogen bonding, the degree of coupling between P and Tp disks was found important for the supramolecular self-assembly in P(Tp)₂ supermolecular crystals.

Results and Discussion

Compounds **1–4** were synthesized following a four-step procedure (Scheme 1). Details and nuclear magnetic resonance (NMR) characterization data are provided in the Experimental Section below. The purity of all samples was confirmed by thin-layer chromatography and size-exclusion chromatography (SEC), and narrow unimodal peaks [polydispersity indices (PDI)=1.01] were obtained (see Figure 1).



Scheme 1. Synthesis of P(Tp)₂ triads with different spacer and alkyl chain lengths.

Abstract in Chinese:

一系列由卟啉和苯并菲构成的线性盘状三联体超分子通过酰胺键连接合成, 样品被标记为 P(Tp)₂。沿着卟啉堆砌方向的氢键被认为是盘状三联体超分子自组装的主要动力。同时, 盘状卟啉和苯并菲的偶合作用也对其自组装有很大的影响。对于间隔基长度大于或相近与苯并菲烷基链长的样品, 卟啉和苯并菲在很大程度上没有偶合作用。因此, 这导致了卟啉和苯并菲沿着 a 轴和 c 轴堆砌方向倾斜角的非均一性, 并且 8 个三联体超分子构成一个大晶包。对于间隔基长度远小于苯并菲烷基链长的样品, 卟啉和苯并菲的紧密偶合作用导致了卟啉和苯并菲沿着 a 轴和 c 轴堆砌方向倾斜角的均一性, 并且一个三联体超分子构成一个小晶包。

Thermal Behaviors and Morphology of P(Tp)₂ Triads

Phase transitions in samples **1–4** were first studied by differential scanning calorimetry DSC (see Figure 2), and results are summarized in Table 1. Sample **1** showed a single crystallization temperature (*T_c*) at 185°C (60 kJ mol⁻¹) upon cooling and a single melting temperature (*T_m*) at 242°C (61 kJ mol⁻¹) upon heating at 10°Cmin⁻¹. Sample **2** showed a different thermal behavior from sample **1**. During the first cooling, it only exhibited a glass transition temperature (*T_g*) at 45°C. Upon the second heating, sample **2** showed a *T_g* at 53°C, a cold crystallization temperature at 131°C (33.5 kJ mol⁻¹), and a *T_m* at 204°C (52 kJ mol⁻¹). Judging from heats of transition and large undercoolings ($\Delta T =$

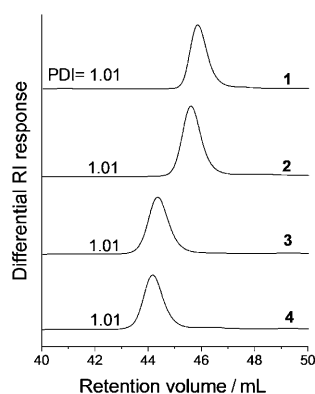


Figure 1. SEC differential refractive index (RI) curves for P(Tp)₂ triads 1–4. Polydispersity indices (PDI) are also shown for all the samples.

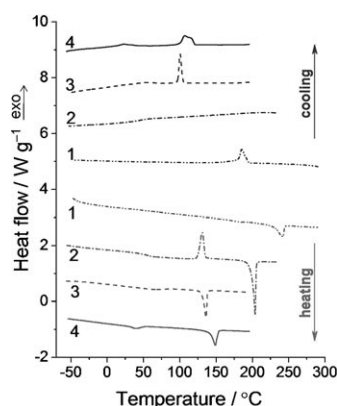


Figure 2. Differential scanning calorimetry (DSC) first cooling and second heating curves for P(Tp)₂ triads 1–4. The scanning rate is 10 °C min⁻¹.

Table 1. Phase transition temperatures (°C, above the arrow) and heats of transition (kJ mol⁻¹, below the arrow) for P(Tp)₂ triads 1–4. Cr = crystal; g = glass; I = isotropic.

Sample	First cooling	First heating
1	I $\xrightarrow{185}$ Cr 60	Cr $\xrightarrow{242}$ I 61
2	I $\xrightarrow{45}$ g	g $\xrightarrow{53}$ I $\xrightarrow{131}$ Cr $\xrightarrow{204}$ I 33.5 52
3	I $\xrightarrow{101}$ Cr ₁ $\xrightarrow{57}$ Cr ₂ 38.8 15.6	Cr ₂ $\xrightarrow{69}$ Cr ₁ $\xrightarrow{136}$ I 21.3 40
4	I $\xrightarrow{107}$ Cr ₁ $\xrightarrow{23}$ Cr ₂ 70 27.2	Cr ₂ $\xrightarrow{39}$ Cr ₁ $\xrightarrow{149}$ I 31.9 72.8

$T_m - T_c$), samples 1 and 2 should be crystalline below the T_m . As shown in the polarized light microscopy (PLM) micrographs for samples 1 and 2 (Figure 3 A and B, respectively), ribbon-like, rather than spherulitic, crystalline morphology was observed.

Samples 3 and 4 exhibited more complex phase behaviors. For example, upon cooling, sample 3 showed a sharp T_c at 101 °C (38.8 kJ mol⁻¹) and a broad peak at 57 °C (15.6 kJ mol⁻¹). Upon heating, two reverse processes took place at 69 °C (21.3 kJ mol⁻¹) and 136 °C (40 kJ mol⁻¹), re-

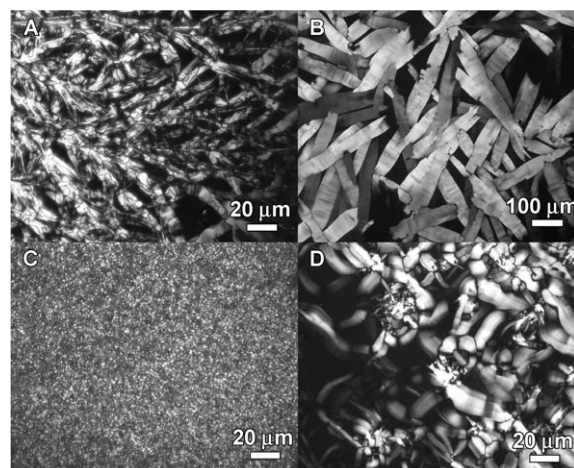


Figure 3. PLM micrographs of P(Tp)₂ triads (A) 1 at 120 °C, (B) 2 at room temperature, (C) 3 at 50 °C, and (D) 4 at room temperature.

spectively. Sample 4 showed a T_c at 107 °C (70 kJ mol⁻¹) and a broad weak peak at 23 °C (27.2 kJ mol⁻¹) during cooling. Upon heating, two reverse processes were observed with a relatively broad peak at 39 °C (31.9 kJ mol⁻¹) and a sharp T_m at 149 °C (72.8 kJ mol⁻¹). Judging from the magnitude of heats of transitions, the high temperature (e.g., 90 °C) phases should be crystalline. On the basis of our previous study,^[64] the low temperature phase transitions could be attributed to the C12 alkyl chain-induced crystallization. The PLM micrograph of sample 4 at room temperature (Figure 3D) showed a sheet-like crystalline texture, which was similar to those of samples 1 and 2. However, sample 3 exhibited a much different morphology from the other three samples, showing an irregular texture with fairly small grains.

Hydrogen Bonding-Induced Supramolecular Self-Assembly in Linear Amide-Linked P(Tp)₂ Triads

The role of hydrogen bonding in the supramolecular self-assembly of amide-linked P(Tp)₂ supermolecules was investigated by temperature-dependent Fourier transform infrared (FTIR) studies, and results are shown in Figure 4A–D for samples 1–4, respectively. Below the T_m , hydrogen-bonded N–H stretching and amide I C=O stretching absorption bands were observed at 3318 and 1641 cm⁻¹, respectively. The appearance of the amide I band at 1641 cm⁻¹ was consistent with a *trans* amide conformation. Above the T_m , the intensity of hydrogen-bonded N–H and amide I bands substantially decreased. Meanwhile, new broad absorption bands appeared at 3415 and 1671 cm⁻¹, which could be assigned to non-hydrogen-bonded N–H and amide C=O absorption bands. We therefore conclude that hydrogen-bonding is the primary driving force for the supramolecular self-assembly of samples 1–4 below their T_m .

The direction of hydrogen-bonding in the P(Tp)₂ samples was studied by polarized FTIR at room temperature. Repre-

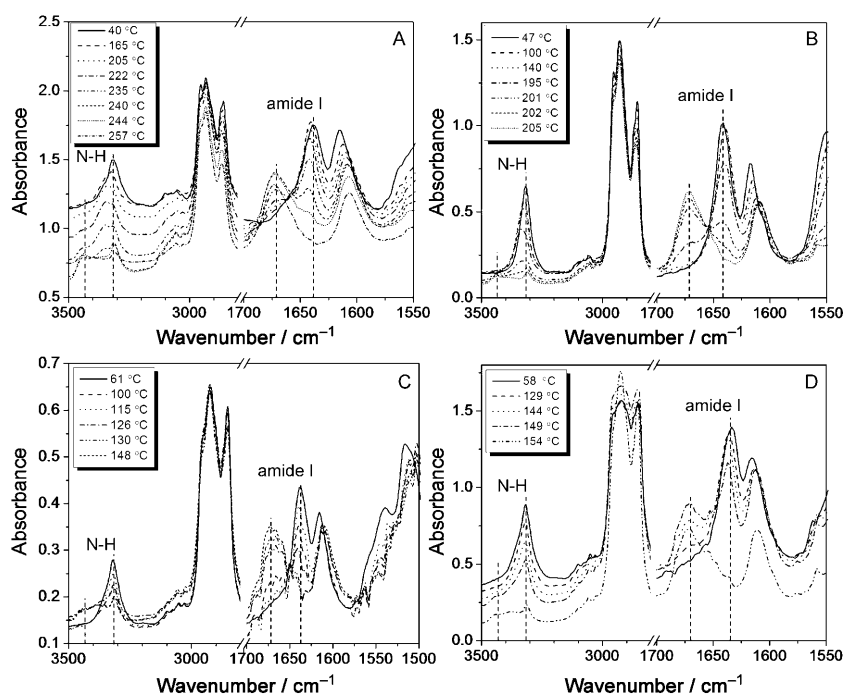


Figure 4. Temperature-dependent FTIR spectra for P(Tp)₂ triads (A) **1**, (B) **2**, (C) **3**, and (D) **4**, respectively.

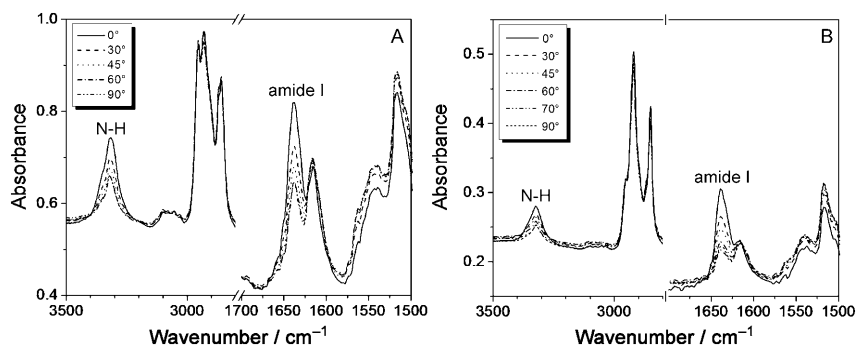


Figure 5. Angle-dependent FTIR spectra for P(Tp)₂ samples (A) **1** and (B) **3**, respectively.

representative results for samples **1** and **3** are shown in Figure 5 A and B, respectively. Samples were shear-oriented on KBr plates at a temperature ca. 20 °C below the T_m using a spatula. The 0°-angle was defined as the polarization plane parallel to the shear direction. Obviously, the amide I and the N-H absorption bands at 1635 and 3326 cm⁻¹ were the strongest when the angle was 0° and weakest when the angle was 90°, suggesting that the hydrogen bonds were along the shear direction. From the XRD analysis below, the shear direction was along the stacking direction of the discotic Ps. Therefore, we conclude that the hydrogen bonds were along the stacking direction of the discotic P molecules.

To exclude the possibility of either J- or H-type of dimers induced by direct π - π stacking between P and Tp, we performed a UV/Vis study of sample **2**, an organo-soluble porphyrin, and the corresponding Tp monoamine (see Figure S1 in the Supporting Information). Basically, the UV/Vis spec-

trum of sample **2** was a linear addition of those of the organo-soluble porphyrin and Tp monoamine. Therefore, we conclude that the direct π - π interaction between P and Tp was not important for the self-assembly of P(Tp)₂ triad supermolecules.

Hydrogen Bond-Assisted Lamellar Structures in P(Tp)₂ Supermolecules

To solve the crystalline structures for P(Tp)₂ supermolecules, 2D XRD experiments were performed on shear-oriented samples and shear temperatures were chosen to be 20 °C below the T_m . To make sure that mechanical shear did not change the phase structure and phase transition, DSC was used to double check the samples before and after shear. On the basis of DSC results for both sheared and unsheared samples (see Figure S2 in the Supporting Information), no substantial effect was observed.

All the 2D XRD patterns in Figure 5 can be explained by an orthorhombic symmetry, and the assigned Miller indices are shown in Figure 6 A–D. The unit cell dimensions are determined as:

- 1) $a = 7.16$ nm, $b = 1.93$ nm, and $c = 1.87$ nm for sample **1**;
- 2) $a = 9.30$ nm, $b = 1.85$ nm, and $c = 1.74$ nm for sample **2**;
- 3) $a = 5.02$ nm, $b = 2.26$ nm, and $c = 0.511$ nm for sample **3**;
- 4) $a = 9.13$ nm, $b = 2.11$ nm, and $c = 2.35$ nm for sample **4**.

The d -spacings of observed XRD reflections fit well to those of calculated values, as demonstrated in Tables S1–S4 in the Supporting Information.

Considering that the molecular weight of sample **1** was 2,247 gmol⁻¹ and the measured density was 1.120 gm⁻³, each unit cell should have eight P(Tp)₂ supermolecules to match the theoretical density of 1.156 gm⁻³. To determine the exact molecular packing inside this orthorhombic unit cell, one needed to perform single crystal XRD studies. Unfortunately, sufficiently large single crystals could not be obtained, possibly as a result of too many alkyl chains in the sample. Therefore, we propose a reasonable packing model within the unit cell based on the molecular sizes as shown in

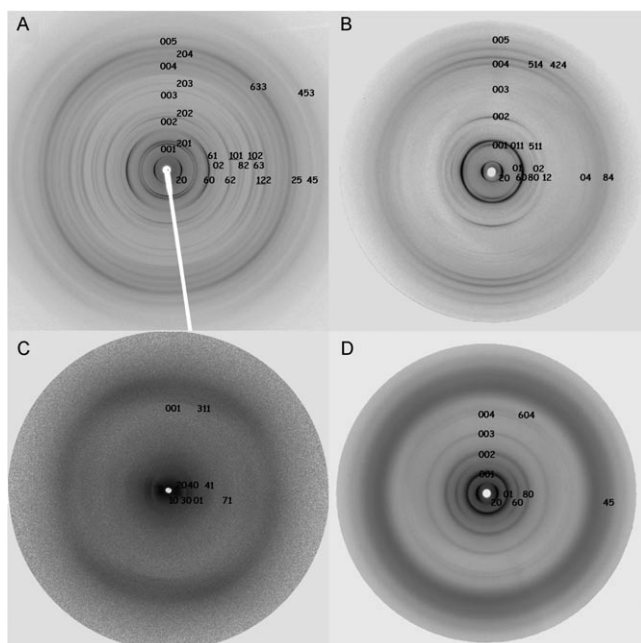


Figure 6. 2D XRD patterns for shear-oriented P(Tp)₂ (A) sample **1** at room temperature; (B) sample **2** 100°C; (C) sample **3** at 110°C, and (D) sample **4** at room temperature.

Figure 7; P–1.99 nm,^[64] C5Tp–1.7 nm,^[65] and C12Tp–2.5 nm.^[66] When we consider eight supermolecules in a unit cell, the *a*-axis should accommodate two P(Tp)₂ supermolecules. However, the *a*-axis (7.16 nm) was smaller than twice the total planar length of the supermolecule (2 × 5.4 =

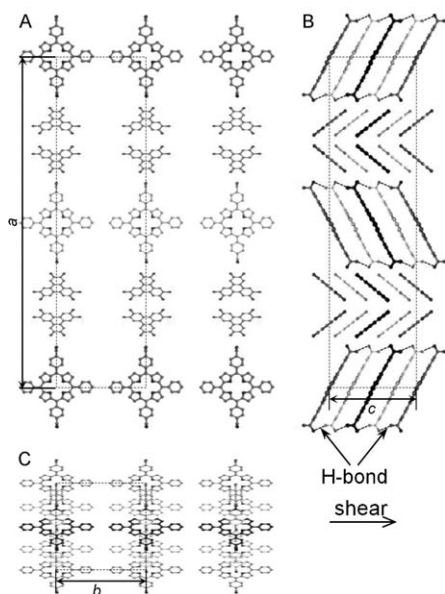


Figure 7. Schematic representation of the packing model for P(Tp)₂ samples **1**, **2** and **4** with three orthogonal view angles (A–C). Both P and Tp are tilted with respect to the *a*-axis. Along the *c*-axis in (B), different colors in P and Tp molecules represent different tilt angles and thus four molecules form a repeat.

10.8 nm). Therefore, the P(Tp)₂ supermolecules should tilt at an angle with respect to the *a*-axis (see Figure 7). Because the spacer length (C6) was longer than the C5 alkyl chain length in the Tp arms, the P and Tp disks were decoupled. Two consequences resulted; (1) The tilt angles for P and Tp might be different. (2) Neighboring P and Tp disks along the *c*-axis might have different tilt angles with four molecules forming a regular motif (see Figure 7). In this model, the hydrogen bonds were along the *c*-axis, which was parallel to the shear direction, consistent with the polarized FTIR results discussed before.

This molecular packing scheme also applies for samples **2** and **4** because their unit cell dimensions are similar to that for sample **1**. Experimental densities for samples **2** and **4** were 1.025 and 0.937 g cm⁻³, again suggesting eight supermolecules per unit cell. Therefore, theoretical densities for samples **2** and **4** are 1.041 and 0.963 g cm⁻³, respectively.

For sample **3**, the observed *a*- and *c*-axes were only 5.02 and 0.511 nm, respectively, much smaller than those (*a* = 9.3 nm and *c* = 2.35 nm) for sample **4**. Considering that the spacer length C6 in sample **3** is shorter than the alkyl chain length of C12 in the Tp arms, P and Tp are strongly coupled together, and thus P disks do not tilt along the *a*-axis in order to form regular π–π stacks (see Figure 8). Assuming

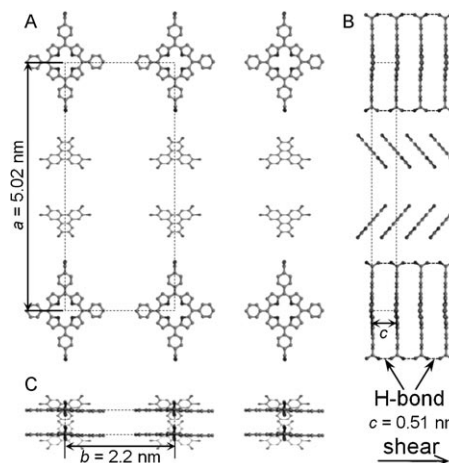


Figure 8. Schematic representation of the packing model for P(Tp)₂ sample **3** with three orthogonal view angles (A–C). Only Tp is tilted along the *a*-axis, and *c*-axis is thus 0.511 nm.

the C12Tp diameter is 2.5 nm,^[66] the tilt angle for the Tp is calculated to be ca. 53°. The measured density was 0.904 g cm⁻³, suggesting only one supermolecule per unit cell. The theoretical density was calculated to be 0.92 g cm⁻³, which is close to the observed one.

Figure 9 shows the 1D XRD profiles for samples **3** and **4** above and below the low temperature transitions. Obviously, the low angle reflections remained the same before and after the low temperature transitions for both samples, indicating that C12 alkyl chain crystallization did not disrupt the pre-existing crystalline structure. However, the amorphous halos at high angles shifted to even higher *q*-values after

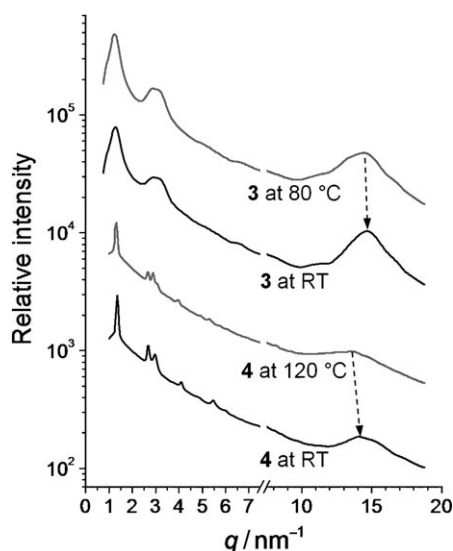


Figure 9. Temperature-dependent 1D XRD profiles for samples **3** and **4**, respectively.

cooling below the low temperature transitions, suggesting a decrease in the average distance among alkyl chains induced by the C12 crystallization.^[64]

Conclusions

In summary, we have successfully synthesized a series of doubly discotic P(Tp)₂ triad supermolecules with amide linkages. Hydrogen bonding along the P stacks was responsible for the supramolecular self-assembly. Besides hydrogen bonding, the coupling between P and Tp disks was also an important factor for the supramolecular self-assembly of P(Tp)₂ supermolecules. For samples **1**, **2**, and **4**, the spacer lengths were longer than or similar to the alkyl chain lengths in the Tp arms, and thus P and Tp were decoupled to a large degree. This decoupling resulted in non-uniform tilt angles for P and Tp disks along both the *a*- and *c*-axes. Therefore, large unit cells with eight P(Tp)₂ supermolecules per cell were observed. For the sample **3**, the spacer was much shorter than the C12 alkyl arms in the Tp arms, and P and Tp were strongly coupled. Therefore, both P and Tp had uniform tilt angles along both the *a*- and *c*-axes. A small unit cell with only one P(Tp)₂ supermolecule per cell was obtained.

Experimental Section

Materials

Methyl-4-formylbenzoate was purchased from TCI America, Inc. Benzo-triazol-1-yl-oxytripyrrolidinophosphonium hexafluorophosphate (PyBOP) and *N,N*-diisopropylethylamine (NPr₂Et) were purchased from Aldrich. Pyrrole, benzaldehyde, boron trifluoride etherate (BF₃·Et₂O), *p*-chloranil, trifluoroacetic acid (TFA), and all solvents were from Fisher

Scientific and used without further purification. Tp mono-amine was prepared according to the literature with slight modifications.^[62]

Instrumentation and Characterization

¹H NMR spectra were recorded on a Bruker spectrometer (500 MHz, DMX 500). DSC experiments were carried out on a TA DSC-Q100 instrument. An indium standard was used for both temperature and enthalpy calibrations. Approximately, 1–3 mg sample was used for the DSC study and the scanning rate was 10 °C min⁻¹. SEC was performed on a Viscotek GPCmax VE2001 with quadruple detectors. THF was used as the solvent and polystyrene standards were used for calibration. PLM experiments were performed using an Olympus BX51P microscope equipped with an Instec HCS410 hot stage. FTIR was performed on a Nicolet Magna 560 FTIR spectrometer.

Two-dimensional (2D) X-ray diffraction (XRD) experiments were performed at the synchrotron X-ray beamline X27C at National Synchrotron Light Source (NSLS), Brookhaven National Laboratory (BNL). The wavelength of incident X-ray was 0.1371 nm. The scattering angle was calibrated using silver behenate with the primary reflection peak at the scattering vector $q = (4\pi \sin \theta) / \lambda = 1.076 \text{ nm}^{-1}$, where θ is the half-scattering angle and λ is the wavelength. Fuji imaging plates were used as detectors for XRD experiments, and digital images were obtained using a Fuji BAS-2500 scanner. The typical data requisition time was 1 min. An Instec HCS410 hot stage equipped with a liquid-nitrogen cooling accessory was used for temperature-dependant X-ray experiments. One-dimensional (1D) XRD curves were obtained by integration of the corresponding 2D XRD patterns.

General Synthesis Procedure and Characterization for Samples 1–4^[64,67]

A solution of methyl-4-formylbenzoate (3 g, 18.4 mmol) in pyrrole (17.4 mL, 250 mmol) was degassed by bubbling dry N₂ for 2 h. After adding 0.11 mL of TFA (1.4 mmol) to the degassed solution, it was stirred at room temperature in the dark for 4 h. The reaction mixture was diluted with 200 mL of CHCl₃ and washed with 0.1 M aqueous NaOH solution and double distilled water successively. The organic layer was dried over anhydrous Na₂SO₄, and the solvent and the excess of pyrrole were removed under a reduced pressure to afford a viscous brown oil which solidified after 12 h. The dry solid was dissolved in a minimum amount of CHCl₃ and loaded on top of a SiO₂ column and eluted by pure CHCl₃. The first brown fraction, which was unreacted pyrrole, was recovered. The later pale yellow fraction was collected and the solvent was removed using a rotary evaporator at room temperature. The resulting pale grey solid was washed with 50 mL of cold ethyl acetate and finally 4.9 g product was obtained (45% yield). ¹H NMR (500 MHz, CDCl₃): δ = 3.90 (s, 3H, COOCH₃), 5.51 (s, 1H, Φ -CH), 5.92 (m, 2H, NH), 6.20 (d, 2H, pyrrole C-CH), 6.75 (d, 2H, NH-CH), 7.25 (t, 2H, NH-CH-CH), and 8.0 ppm (d, 4H, Φ -H).

A solution of dipyrrole (3 g, 10.7 mmol) and benzaldehyde (1.13 g, 10.7 mmol) in 400 mL of CHCl₃ was degassed by bubbling N₂ for 2 h. Following the addition of BF₃·Et₂O (1.37 mL, 10.7 mmol) to the degassed solution, the reaction mixture was stirred at room temperature in the dark for 2 h. Subsequently, *p*-chloranil (4.5 g, 19 mmol) was added to the resulting dark red solution. After stirring overnight, 5 mL of triethylamine (38 mmol) was added to the reaction mixture to neutralize the Lewis acid. The crude reaction mixture was then concentrated and loaded on a SiO₂ flash column using CHCl₃ as the eluent. The obtained purple solution was evaporated to afford a mixture of porphyrins which was further subject to column chromatography (SiO₂, hexanes/toluene = 2:1 to 1:3). The desired *para*-substituted porphyrin dicarboxylates were obtained right before the *ortho*-substituted isomers. After removing the *ortho*-substituted isomer, the desired *para*-substituted porphyrin dicarboxylate was obtained as a later fraction. After evaporating the solvent, a purple solid was obtained (0.6 g, 10% yield). ¹H NMR (500 MHz, CDCl₃): δ = 4.12 (s, 6H, COOCH₃), 7.81 (m, 6H, 3,4,5- Φ -H in non-ester functionalized phenyl rings), 8.25 (m, 4H, 2,6- Φ -H in non-ester functionalized phenyl rings), 8.33 (m, 4H, 2,6- Φ -H in ester functionalized phenyl ring), 8.49 (m, 4H, 3,5- Φ -H in ester functionalized phenyl ring), 8.79 (m,

4H, P-H close to non-ester functionalized phenyl ring), and 8.90 ppm (m, 4H, P-H close to ester functionalized phenyl ring).

The *para*-substituted porphyrin dicarboxylate (0.6 g, 1.05 mmol) was dissolved in 200 mL of tetrahydrofuran (THF)/methanol (1:1 vol/vol) mixture, and KOH (3 g) in 30 mL of H₂O was added to carry out the hydrolysis reaction under reflux for 12 h. After cooling to ambient temperature, the organic solvent was removed under a reduced pressure, and the residue was diluted with 100 mL of water. The resulting dipotassium salt of the corresponding porphyrin dicarboxylic acid was collected by filtration. The solid dipotassium salt was acidified with concentrated HCl, followed by a thorough wash with hot water. Finally, a purple powder of the porphyrin dicarboxylic acid (570 mg, 96% yield) was obtained. ¹H NMR (500 MHz, [D₆]DMSO): δ = 7.03 (brm, 6H, 3,4,5- Φ -H in non-ester functionalized phenyl ring), 7.26 (brs, 4H, 2,6- Φ -H in non-ester functionalized phenyl ring), 7.52 (m, 4H, 2,6- Φ -H in ester functionalized phenyl ring), 7.64 (m, 4H, 3,5- Φ -H in ester functionalized phenyl ring), 8.05 (brs, 4H, P-H close to non-ester functionalized phenyl ring), and 8.12 ppm (brs, 4H, P-H close to ester functionalized phenyl ring).

100 mg (0.14 mmol) of porphyrin dicarboxylic acid was activated by 200 mg (0.35 mmol) of PyBOP and 2 drops of NPr₂Et in 5 mL of anhydrous *N,N*-dimethylformamide (DMF). The mixture solution was sonicated for 10 min at room temperature, followed by addition of 0.35 mmol (270 mg for **1**, 290 mg for **2**, 443 mg for **3**, and 462 mg for **4**, see chemical structures in Scheme 1) of the corresponding triphenylene mono-amine. The reaction mixture was further sonicated at room temperature for 30 min. The completion of reaction was checked by thin layer chromatography (TLC) using CHCl₃ as the developing solvent. The reaction mixture was then poured into 20 mL of double-distilled water and triply extracted with 10 mL of CHCl₃ each time. The combined organic fractions were washed with 20 mL of 1 N HCl, 20 mL of 0.7 N NaHCO₃, and 20 mL of brine, before drying over anhydrous MgSO₄. After filtration and removal of the solvent under vacuum, crude products were purified by column chromatography (silica gel, gradient hexane to chloroform/hexane 95:5). Purple solids were obtained with yields: 43% for **1** (135 mg), 39% for **2** (129 mg), 19% for **3** (85 mg), and 12% for **4** (56 mg).

¹H NMR for **1**, (CDCl₃): δ = 1.0–0.85 (30H, m, CH₃), 2.0–1.2 (76H, m, CH₂ in alkyl tails), 3.58 (4H, m, CH₂NHCO), 4.3–4.15 (24H, m, ArOCH₂), 6.51 (2H, m, NHCO), 7.9–7.7 (18H, m, Tp-H, P phenyl Φ -H), 8.4–8.1 (12H, m, P phenyl Φ -H), 9.0–8.8 ppm (8H, m, P pyrrole P-H). ¹³C NMR for **1**, (CDCl₃): δ = 14.1, 22.6, 28.4, 29.1, 40.3, 69.6, 107.3, 118.9, 120.5, 123.6, 125.3, 126.7, 127.8, 134.5, 134.7, 141.9, 145.3, 149.0, 167.7 ppm.

¹H NMR for **2**, (CDCl₃): δ = 1.0–0.85 (30H, m, CH₃), 2.0–1.2 (92H, m, CH₂ in alkyl tails), 3.62 (4H, m, CH₂NHCO), 4.3–4.15 (24H, m, ArOCH₂), 6.43 (2H, m, NHCO), 7.9–7.7 (18H, m, Tp-H, P phenyl Φ -H), 8.4–8.1 (12H, m, P phenyl Φ -H), 9.0–8.8 ppm (8H, m, P pyrrole P-H). ¹³C NMR for **2**, (CDCl₃): δ = 14.1, 22.6, 28.4, 29.1, 40.3, 69.6, 107.3, 118.9, 120.5, 123.6, 125.3, 126.7, 127.8, 134.5, 134.7, 141.9, 145.3, 149.0, 167.7 ppm.

¹H NMR of **3**, (CDCl₃): δ = 1.0–0.85 (30H, m, CH₃), 2.0–1.2 (216H, m, CH₂ alkyl tails), 3.61 (4H, m, CH₂NHCO), 4.3–4.15 (24H, m, ArOCH₂), 6.51 (2H, m, NHCO), 7.9–7.7 (18H, m, Tp-H, P phenyl Φ -H), 8.4–8.1 (12H, m, P phenyl Φ -H), 9.0–8.8 ppm (8H, m, P pyrrole P-H). ¹³C NMR for **3**, (CDCl₃): δ = 14.1, 22.7, 26.2, 29.5, 29.7, 31.9, 40.3, 69.7, 107.4, 118.9, 120.5, 123.6, 125.3, 126.7, 127.8, 134.7, 141.9, 145.4, 149.0, 167.6 ppm.

¹H NMR of **4**, (CDCl₃): δ = 1.0–0.85 (30H, m, CH₃), 2.0–1.2 (232H, m, CH₂ in alkyl tails), 3.61 (4H, m, CH₂NHCO), 4.3–4.15 (24H, m, ArOCH₂), 6.45 (2H, m, NHCO), 7.9–7.7 (18H, m, Tp-H, P phenyl Φ -H), 8.4–8.1 (12H, m, P phenyl Φ -H), 9.0–8.8 ppm (8H, m, P pyrrole P-H). ¹³C NMR for **4**, (CDCl₃): δ = 14.1, 22.7, 26.2, 29.5, 29.7, 31.9, 40.3, 69.7, 107.4, 118.9, 120.5, 123.6, 125.3, 126.7, 127.8, 134.7, 141.9, 145.4, 149.0, 167.6 ppm.

Acknowledgements

This work was supported by NSF CAREER Award DMR-0348724, DuPont Young Professor Grant, and 3M Nontenured Faculty Award. The synchrotron X-ray experiments were carried out at the National Synchrotron Light Source, Brookhaven National Laboratory, which is supported by the U.S. Department of Energy. Assistance from Drs. Lixia Rong and Jie Zhu, and Prof. Benjamin Hsiao at State University of New York at Stony Brook for synchrotron X-ray experiments is highly acknowledged.

- [1] J.-M. Lehn, *Supramolecular Chemistry: Concepts and Perspectives*, VCH, New York, **1995**.
- [2] I. M. Saez, J. W. Goodby, *J. Mater. Chem.* **2005**, *15*, 26–40.
- [3] T. Kato, N. Mizoshita, K. Kishimoto, *Angew. Chem.* **2006**, *118*, 44–74; *Angew. Chem. Int. Ed.* **2006**, *45*, 38–68.
- [4] V. Percec, M. Glodde, T. K. Bera, Y. Miura, I. Shiyonovskaya, K. D. Singer, V. S. K. Balagurusamy, P. A. Heiney, I. Schnell, A. Rapp, H. W. Spiess, S. D. Hudson, H. Duan, *Nature* **2002**, *417*, 384–387.
- [5] V. Percec, A. E. Dulcey, V. S. K. Balagurusamy, Y. Miura, J. Smidral, M. Peterca, S. Nummelin, U. Edlund, S. D. Hudson, P. A. Heiney, D. A. Hu, S. N. Magonov, S. A. Vinogradov, *Nature* **2004**, *430*, 764–768.
- [6] V. Percec, A. E. Dulcey, M. Peterca, M. Ilies, M. J. Sienkowska, P. A. Heiney, *J. Am. Chem. Soc.* **2005**, *127*, 17902–17909.
- [7] V. Percec, M. Glodde, M. Peterca, A. Rapp, I. Schnell, H. W. Spiess, T. K. Bera, Y. Miura, V. S. K. Balagurusamy, E. Aqad, P. A. Heiney, *Chem. Eur. J.* **2006**, *12*, 6298–6314.
- [8] V. Percec, A. E. Dulcey, M. Peterca, M. Ilies, S. Nummelin, M. J. Sienkowska, P. A. Heiney, *Proc. Natl. Acad. Sci. USA* **2006**, *103*, 2518–2523.
- [9] M. Peterca, V. Percec, A. E. Dulcey, S. Nummelin, S. Korey, M. Ilies, P. A. Heiney, *J. Am. Chem. Soc.* **2006**, *128*, 6713–6720.
- [10] K. Lorenz, D. Holter, B. Stuhn, R. Mulhaupt, H. Frey, *Adv. Mater.* **1996**, *8*, 414–416.
- [11] M. Baars, S. H. M. Sontjens, H. M. Fischer, H. W. I. Peerlings, E. W. Meijer, *Chem. Eur. J.* **1998**, *4*, 2456–2466.
- [12] J. Barberá, M. Marcos, J. L. Serrano, *Chem. Eur. J.* **1999**, *5*, 1834–1840.
- [13] M. Marcos, R. Gimenez, J. L. Serrano, B. Donnio, B. Heinrich, D. Guillon, *Chem. Eur. J.* **2001**, *7*, 1006–1013.
- [14] B. Donnio, J. Barbera, R. Gimenez, D. Guillon, M. Marcos, J. L. Serrano, *Macromolecules* **2002**, *35*, 370–381.
- [15] S. A. Ponomarenko, N. I. Boiko, V. P. Shibaev, R. M. Richardson, I. J. Whitehouse, E. A. Rebrov, A. M. Muzafarov, *Macromolecules* **2000**, *33*, 5549–5558.
- [16] J. M. Rueff, J. Barbera, M. Marcos, A. Omenat, R. Martin-Rapun, B. Donnio, D. Guillon, J. L. Serrano, *Chem. Mater.* **2006**, *18*, 249–254.
- [17] J. H. Cameron, A. Facher, G. Lattermann, S. Diele, *Adv. Mater.* **1997**, *9*, 398–403.
- [18] K. U. Jeong, A. J. Jing, B. Mansdorf, M. J. Graham, D. K. Yang, F. W. Harris, S. Z. D. Cheng, *Chem. Mater.* **2007**, *19*, 2921–2923.
- [19] C. T. Imrie, Z. B. Lu, S. J. Picken, Z. Yildirim, *Chem. Commun.* **2007**, 1245–1247.
- [20] A. M. Levelut, K. Moriya, *Liq. Cryst.* **1996**, *20*, 119–124.
- [21] K. Moriya, T. Suzuki, S. Yano, S. Miyajima, *J. Phys. Chem. B* **2001**, *105*, 7920–7927.
- [22] J. Barberá, M. Bardaji, J. Jimenez, A. Laguna, M. P. Martinez, L. Oriol, J. L. Serrano, I. Zaragoza, *J. Am. Chem. Soc.* **2005**, *127*, 8994–9002.
- [23] J. Barberá, J. Jimenez, A. Laguna, L. Oriol, S. Perez, J. L. Serrano, *Chem. Mater.* **2006**, *18*, 5437–5445.
- [24] B. Dardel, R. Deschenaux, M. Even, E. Serrano, *Macromolecules* **1999**, *32*, 5193–5198.
- [25] T. Chuard, R. Deschenaux, A. Hirsch, H. Schonberger, *Chem. Commun.* **1999**, 2103–2104.

- [26] D. Felder-Flesch, L. Rupnicki, C. Bourgoigne, B. Donnio, D. Guillon, *J. Mater. Chem.* **2006**, *16*, 304–309.
- [27] G. H. Mehl, J. W. Goodby, *Angew. Chem.* **1996**, *108*, 2791–2793; *Angew. Chem. Int. Ed. Engl.* **1996**, *35*, 2641–2643.
- [28] J. W. Goodby, G. H. Mehl, I. M. Saez, R. P. Tuffin, G. Mackenzie, R. Auzely-Velty, T. Benvegno, D. Plusquellec, *Chem. Commun.* **1998**, 2057–2070.
- [29] R. Elsässer, G. H. Mehl, J. W. Goodby, D. J. Photinos, *Chem. Commun.* **2000**, 851–852.
- [30] I. M. Saez, J. W. Goodby, *J. Mater. Chem.* **2001**, *11*, 2845–2851.
- [31] I. M. Saez, J. W. Goodby, R. M. Richardson, *Chem. Eur. J.* **2001**, *7*, 2758–2764.
- [32] R. M. Laine, C. X. Zhang, A. Sellinger, L. Viculis, *Appl. Organomet. Chem.* **1998**, *12*, 715–723.
- [33] C. X. Zhang, T. J. Bunning, R. M. Laine, *Chem. Mater.* **2001**, *13*, 3653–3662.
- [34] P. K. Karahaliou, P. H. J. Kouwer, T. Meyer, G. H. Mehl, D. J. Photinos, *Soft Matter* **2007**, *3*, 857–865.
- [35] P. K. Karahaliou, P. H. J. Kouwer, T. Meyer, G. H. Mehl, D. J. Photinos, *J. Phys. Chem. B* **2008**, *112*, 6550–6556.
- [36] Q. W. Pan, X. F. Chen, X. G. Fan, Z. H. Shen, Q. F. Zhou, *J. Mater. Chem.* **2008**, *18*, 3481–3488.
- [37] C. T. Imrie, P. A. Henderson, *Curr. Opin. Colloid Interface Sci.* **2002**, *7*, 298–311.
- [38] C. T. Imrie, P. A. Henderson, G. Y. Yeap, *Liq. Cryst.* **2009**, *36*, 755–777.
- [39] N. Boden, R. J. Bushby, A. N. Cammidge, P. S. Martin, *J. Mater. Chem.* **1995**, *5*, 1857–1860.
- [40] W. Kranig, B. Huser, H. W. Spiess, W. Kreuder, H. Ringsdorf, H. Zimmerman, *Adv. Mater.* **1990**, *2*, 36–40.
- [41] S. K. Gupta, V. A. Raghunathan, S. Kumar, *New J. Chem.* **2009**, *33*, 112–118.
- [42] M. D. McKenna, J. Barbera, M. Marcos, J. L. Serrano, *J. Am. Chem. Soc.* **2005**, *127*, 619–625.
- [43] S. Kumar, M. Manickam, *Liq. Cryst.* **1999**, *26*, 939–941.
- [44] A. Grafe, D. Janietz, T. Frese, J. H. Wendorff, *Chem. Mater.* **2005**, *17*, 4979–4984.
- [45] N. C. Maliszewskij, P. A. Heiney, J. Y. Josefowicz, T. Plesniviy, H. Ringsdorf, P. Schuhmacher, *Langmuir* **1995**, *11*, 1666–1674.
- [46] H. K. Bisoyi, S. Kumar, *Tetrahedron Lett.* **2008**, *49*, 3628–3631.
- [47] T. Plesniviy, H. Ringsdorf, P. Schuhmacher, U. Nuetz, S. Diele, *Liq. Cryst.* **1995**, *18*, 185–190.
- [48] A. Zelcer, B. Donnio, C. Bourgoigne, F. D. Cukiernik, D. Guillon, *Chem. Mater.* **2007**, *19*, 1992–2006.
- [49] L. Zhi, J. Wu, K. Mullen, *Org. Lett.* **2005**, *7*, 5761–5764.
- [50] W. Kreuder, H. Ringsdorf, O. Herrmann-Schönherr, J. H. Waddon, *Angew. Chem.* **1987**, *99*, 1300–1303.
- [51] S. Mahlstedt, D. Janietz, C. Schmidt, A. Stracke, J. H. Wendorff, *Liq. Cryst.* **1999**, *26*, 1359–1369.
- [52] S. Mahlstedt, D. Janietz, A. Stracke, J. H. Wendorff, *Chem. Commun.* **2000**, 15–16.
- [53] Y. Matsunaga, N. Miyajima, Y. Nakayasu, S. Sakai, M. Yonenaga, *Bull. Chem. Soc. Jpn.* **1988**, *61*, 207–210.
- [54] K. Hanabusa, C. Koto, M. Kimura, H. Shirai, A. Kakehi, *Chem. Lett.* **1997**, 429–430.
- [55] M. L. Bushey, A. Hwang, P. W. Stephens, C. Nuckolls, *J. Am. Chem. Soc.* **2001**, *123*, 8157–8158.
- [56] M. L. Bushey, A. Hwang, P. W. Stephens, C. Nuckolls, *Angew. Chem.* **2002**, *114*, 2952–2955; *Angew. Chem. Int. Ed.* **2002**, *41*, 2828–2831.
- [57] A. R. A. Palmans, J. Vekemans, E. E. Havinga, E. W. Meijer, *Angew. Chem.* **1997**, *109*, 2763–2765; *Angew. Chem. Int. Ed. Engl.* **1997**, *36*, 2648–2651.
- [58] J. J. van Gorp, J. Vekemans, E. W. Meijer, *J. Am. Chem. Soc.* **2002**, *124*, 14759–14769.
- [59] M. H. J. Smulders, A. Schenning, E. W. Meijer, *J. Am. Chem. Soc.* **2008**, *130*, 606–611.
- [60] M. L. Bushey, T. Q. Nguyen, C. Nuckolls, *J. Am. Chem. Soc.* **2003**, *125*, 8264–8269.
- [61] T. Q. Nguyen, R. Martel, M. Bushey, P. Avouris, A. Carlsen, C. Nuckolls, L. Brus, *Phys. Chem. Chem. Phys.* **2007**, *9*, 1515–1532.
- [62] I. Paraschiv, M. Giesbers, B. van Lagen, F. C. Grozema, R. D. Abellon, L. D. A. Siebbeles, A. T. M. Marcelis, H. Zuilhof, E. J. R. Sudholter, *Chem. Mater.* **2006**, *18*, 968–974.
- [63] I. Paraschiv, K. de Lange, M. Giesbers, B. van Lagen, F. C. Grozema, R. D. Abellon, L. D. A. Siebbeles, E. J. R. Sudholter, H. Zuilhof, A. T. M. Marcelis, *J. Mater. Chem.* **2008**, *18*, 5475–5481.
- [64] J. Miao, L. Zhu, *Chem. Mater.* **2010**, *22*, 197–206.
- [65] L. Cui, J. P. Collet, G. Q. Xu, L. Zhu, *Chem. Mater.* **2006**, *18*, 3503–3512.
- [66] F. Würthner, C. Thalacker, S. Diele, C. Tschierske, *Chem. Eur. J.* **2001**, *7*, 2245–2253.
- [67] S. Saha, E. Johansson, A. H. Flood, H. R. Tseng, J. I. Zink, J. F. Stoddart, *Chem. Eur. J.* **2005**, *11*, 6846–6858.

Received: January 8, 2010
Published online: May 21, 2010